

# Oxidative Stress Reducing Osteogenesis Reversed by Curcumin via NF- $\kappa$ B Signaling and Had a Role in Anti-Osteoporosis

**Xu JiaQiang**

First Affiliated Hospital of Nanchang University

**Ran Gao**

First Affiliated Hospital of Nanchang University

**Wen Liang**

First Affiliated Hospital of Nanchang University

**ChangJian Wu**

First Affiliated Hospital of Nanchang University

**FangLing Li**

First Affiliated Hospital of Nanchang University

**Sheng Huang**

First Affiliated Hospital of Nanchang University

**Bing Zhang**

First Affiliated Hospital of Nanchang University

**QiHua Qi** (✉ [qqhua1938@126.com](mailto:qqhua1938@126.com))

Department of Orthopedic, The First Affiliated Hospital of Nanchang University, Nanchang, 330006, P R China

---

## Research article

**Keywords:** osteogenesis, oxidative stress, curcumin, osteoporosis, NF- $\kappa$ B

**Posted Date:** April 7th, 2021

**DOI:** <https://doi.org/10.21203/rs.3.rs-362019/v1>

**License:** © ⓘ This work is licensed under a Creative Commons Attribution 4.0 International License.

[Read Full License](#)

---

# Abstract

**Objective:** Curcumin has good anti-inflammatory and antioxidant properties, and whether it can resist osteoporosis through oxidative stress pathway in a dose-dependent manner.

**Method:** we used an oxidative stress cell model by culture cells with hydrogen peroxide ( $H_2O_2$ ), cells were osteogenic differentiation after treated with  $H_2O_2$  different concentration curcumin were added during differentiation, then measured the early and late osteogenic index, and detected the potential signaling pathway involved. In addition, we employed rat OVX model treated with curcumin to confirm the protection of the anti-oxidant.

**Result:** Low concentrations of curcumin (1-10 $\mu$ M) promoted the proliferation of MC3T3-E1 cells, improved alkaline phosphatase (ALP) activity, elevated calcium content against oxidative stress induced by  $H_2O_2$ , but high concentration (20  $\mu$ M) failed, moreover, curcumin diminished supernatant receptor activator of nuclear factor kappa-B ligand (RANKL) and IL-6 expression, inhibited the intracellular ROS triggered by  $H_2O_2$ , Notably, curcumin exerted protection by blocking the NF- $\kappa$ B signaling pathway. The curcumin administered for 12 weeks partially reversed the ratio of blood malondialdehyde (MDA) and glutathione (GSH) activity in ovariectomized (OVX) rat in vivo. It also increased the bone mineral density (BMD) and improved the micro-architecture of trabecular bones.

**Conclusion:** curcumin exerted protection on osteoporosis, the effect linked to a reduction of oxidative stress and bone resorbing cytokine, This study suggests that curcumin might be a candidate for osteoporosis prevention and the low concentration exerted obviously protection.

## Introduction

Osteoporosis influencing millions of people' life quality worldwide, is the most common bone disease in elderly, it affected approximately 34% of women, most of whom are post-menopausal, and 17% of men<sup>[1]</sup>. The osteoporosis is characterized by micro-architectural deterioration of trabecular bone, resulted in bone fragility and susceptibility to fracture consequently, the disease lead to a high medical expenditures and substantial morbidity currently<sup>[2-4]</sup>.

Estrogen deficiency in post-menopausal women was considered as the etio-pathogenesis of osteoporosis in the past decades<sup>[5]</sup>, but now oxidative stress is regarded as the main pathology of osteoporosis<sup>[6, 7]</sup>. Many researchers suggested that the osteopenia of postmenopausal osteoporotic women was related to lowered superoxide dismutase (SOD), glutathione peroxidase and higher oxidation of plasma lipid<sup>[8-11]</sup>. Then, the theory pathogenesis of osteoporosis shifted from the "estrogen-centric" concept to oxidative stress was protagonists.

Bone continuously renews itself throughout one's entire life by the coordinated action of two major types of cells: osteoclasts and osteoblasts, the redox state changes alters bone remodeling process by regulating the balance between osteoclast and osteoblast activity<sup>[12-15]</sup>. ROS induced the apoptosis of

osteoblasts, and reduced their activity, which was detrimental to osteogenesis, and high levels of ROS block and reduce the osteoblast differentiation, then reduced the mineralization and osteogenesis<sup>[16-18]</sup>.

Curcumin, a yellow molecule extracted from curcuma longa and turmeric, have been proved possessed good anti-inflammatory and antioxidant properties<sup>[19, 20][21, 22]</sup> Curcumin has been found to antagonize intracellular ROS and scavenge free radical effectively now<sup>[23-25]</sup>.

Curcumin play a more important role in the relationship between the oxidative stress and osteogenesis. It has reported that curcumin can protect against oxidative injury and promote osteoblast differentiation of MSCs by attenuated the inhibition of Wnt/ $\beta$ -catenin signaling<sup>[26]</sup>. The mitochondrial redox potential was crucial to the fate of the cells, curcumin not only decreased the mitochondrial oxidative status, but also improved the mitochondrial membrane potential, ameliorated oxidative stress-induced apoptosis in osteoblasts<sup>[27]</sup>. Many *in vitro* studies indicate that the proliferation and differentiation of osteoclast triggered by oxidative stress were reversed by curcumin, and ameliorated the bone loss of ovariectomized animals (OVX) *in vivo*<sup>[28, 29]</sup>.

There few studies focus on how the curcumin regulate the oxidative stress and osteoporosis, and, which signaling pathway mainly related to also unclear. The dose dependence relationship between curcumin and the osteoporosis also need to clarify. So, we will examine the anti-oxidative stress effects of curcumin and the underlying mechanisms using an H<sub>2</sub>O<sub>2</sub>-induced oxidative stress model *in vitro* and murine ovariectomized model *in vivo*.

## Materials And Methods

### 2.1 Chemicals and reagents

Curcumin (purity, 98.0%; molecular weight, 368.38; dissolved in distilled water with DMSO) was purchased from Sigma-Aldrich (St. Louis, MO, USA). The R&D systems Inc provided the RANKL and IL-6 ELISA assay kits, (Minneapolis, MN, USA). Antibodies against I $\kappa$ B- $\alpha$ , p-P65,  $\beta$ -actin were obtained from Abcam (Beverly, MA, USA). BCA protein assay kit (Thermo Fisher Scientific, Rockford, IL, USA), the GSH and MDA assay kits and the BCIP/NBT alkaline phosphatase color development kit were purchased from the Beyotime Institute of Biotechnology (Shanghai, China). Other chemicals (dexamethasone,  $\beta$ -glycerophosphate, H<sub>2</sub>O<sub>2</sub>, N-acetyl-L-cysteine (NAC), Alizarin Red S, methylthiazolyltetrazolium (MTS), p-nitrophenylphosphate (pNPP)) were also purchased from Sigma-Aldrich (St. Louis, MO, USA).

### 2.2 Cell culture and treatment

Murine MC3T3-E1 cells were purchased from the American Type Culture Collection (ATCC, Manassas, VA, USA). Cells were cultured in modified  $\alpha$ -MEM medium with 10% heat-inactivated FBS (Gibco Invitrogen, Carlsbad, CA, USA) at 37°C in a humidified 5%CO<sub>2</sub> atmosphere. The medium was replenished every three days. H<sub>2</sub>O<sub>2</sub> used as an exogenous ROS treatment, and N-acetyl-L-cysteine (NAC) served as an

antioxidant. Fresh osteogenic medium (OM, 50 µg/ml ascorbic acid, 10 mM β-glycerophosphate and 0.1 µM dexamethasone), containing different concentrations of curcumin was prepared for osteogenic induction after 0.3 mM H<sub>2</sub>O<sub>2</sub> was administered for 24 h. All of the experiments were conducted in duplicate wells and repeated three times.

### **2.3 Intracellular ROS level and Cell viability assay**

Cells were treated with 0.3mM H<sub>2</sub>O<sub>2</sub> and cultured for 24h. Then the cells were incubated in culture containing 20 µM DCFH-DA for 30 min at 37°C. The cells were then rinsed with PBS to remove the residual extracellular DCFH-DA. The cellular fluorescence was visualized using fluorescence microscopy (Axio Observer Z1, Carl Zeiss Inc.), or the cells were detached with trypsin and resuspended after centrifugation. The fluorescence levels of the samples were measured using flow cytometry with the excitation and emission wavelengths set at 488 and 525 nm, respectively.

Different concentrations of H<sub>2</sub>O<sub>2</sub> (0.1, 0.2, 0.3, 0.5, 1 and 2 mM) were administered in MC3T3-E1 cells for 24h in whole culture. Similarly, different curcumin solution (1, 5, 10, 20, 50, 100 and 200 µM dissolved in 0.1% DMSO in distilled water) was also added to the cell cultures. 0.1% DMSO in distilled water served as control group. The cells were incubated using whole culture medium, which contained curcumin (1, 5, 10, 20, 50, 100 or 200 µM) for 24 h followed by the adding of 300 µM H<sub>2</sub>O<sub>2</sub> for 24 h. The cells were rinsed with PBS once, and then, 120 µl of fresh medium containing 20 µl MTS was added to all wells. After incubation at 37°C for 3 h, the absorbance at 490 nm was measured using a spectrophotometric plate reader.

### **2.4 Alkaline phosphatase (ALP) staining and activity assay**

The murine MC3T3-E1 cells treated with 0.3mM H<sub>2</sub>O<sub>2</sub> for 24 h, and added osteogenic media contained different concentrations of curcumin for 7 days. At 7 days, the cells were lysed with 1% Triton X-100 overnight at 4°C. A portion of the lysate was incubated with p-NPP in a buffer (0.1 M glycine, 1 mM ZnCl<sub>2</sub> and MgCl<sub>2</sub>, pH 10.3) at 37°C for 30 min; the reaction was terminated by 2 M NaOH solution, and the absorbance was measured at 405 nm. The ALP activity was normalized to total protein, and the protein was measured using the Bradford protein assay. The cells were stained followed the instruction of the BCIP/NBT alkaline phosphatase color development kit.

### **2.5 Calcium content assay and alizarin red staining**

The calcium content was measured with a Calcium Assay kit at 21 days according to the manufacturer's instructions. The samples were added with 1 M acetic acid and placed on a vortex overnight at 4°C to extract the calcium. a portion of the extract was mixed with 150 µL Calcium Assay reagent and incubated for 30 s at 37°C. The absorbance at 575 nm was measured using a SpectraMAX 250 microplate reader. The calcium content was normalized to cell total protein. The mineralization was observed using Alizarin Red staining, for Alizarin Red staining, after cells were fixed with 4% paraformaldehyde for 15 min, they stained with 40 mM Alizarin Red S for 15 min at room temperature, distilled water was used to remove

the unbound stain, the cells were visualized and imaged using a light microscope (Nikon, Eclipse TS100, Japan) and digital camera (Nikon, D330, Japan).

## **2.6 RANKL and IL-6 measurements**

After exposure to H<sub>2</sub>O<sub>2</sub> for 24 h, the murine MC3T3-E1 cells were incubated using whole culture medium, which contained three different concentrations (1, 10, and 20 μM) of curcumin for 7 days. The production of RANKL and IL-6 in culture medium was detected using a sandwich ELISA assay kit following the manufacturer's instructions. The total protein concentrations were measured by the Bradford protein assay method.

## **2.7 Western Blot**

After pretreated with curcumin for 24h, the cells were cultured with H<sub>2</sub>O<sub>2</sub> for 1h, Cells were collected, and protein was harvested using RIPA buffer supplemented with a protease inhibitor cocktail (Sigma-Aldrich). The total protein concentration was determined with BCA protein assay kit following the manufacturer's instructions. Thirty micrograms of protein was separated by SDS-PAGE and then transferred onto a 0.45 μm PVDF membrane. The membranes were blocked and then probed overnight with rabbit polyclonal antibodies against p-p65, p-IκBα and β-actin. The antibodies were detected using enhanced chemiluminescence with HRP-conjugated secondary antibodies. The values of the band intensities were quantified using Image J software.

## **2.8 Ovariectomized mouse model and curcumin intervention**

We used an ovariectomized (OVX) mouse model to observe the protective effect of curcumin on the oxidation in vivo, the usage of animals was approved by the Animal Care Committee of the university of Sun Yat-sen (permission code: SYXK2010-0108). Forty 8 weeks old BALB/c female mice, weighing about 20.52 ± 1.27g, were purchased from the experimental animal center of the first affiliated hospital of Sun Yat-sen university (Guangzhou, China). The mice underwent sham (n = 10) or ovariectomy operation (OVX) (n = 30) with anesthesia using sodium pentobarbital (50 mg/kg body weight, i.p.). The ovariectomy operation was performed with dorsal approach. A total of 30 BALB/c female mice were randomly distributed into three groups: 1) an OVX group (vehicle), with DMSO solvent administered intraperitoneally (n = 10); 2) an OVX group (low), with curcumin solution administered intraperitoneally (5 μmol/kg body weight; n = 10) daily; and 3) an OVX group (high), with curcumin solution administered intraperitoneally (15 μmol/kg body weight; n = 10) daily. Curcumin solution was prepared by dissolved in distilled water with DMSO. One week later, the treatments were initiated and continued for 12 weeks. Blood samples were collected from the hearts of the anesthetized mice, and serum samples were harvested by centrifugation. The femurs of the mice were prepared for further bone analysis, and the adherent tissue was discarded completely.

## **2.9 Measurements of serum malondialdehyde (MDA) and glutathione (GSH)**

The MDA activity of the whole blood samples was measured using a MDA assay kit following the manufacturer's instructions. Thiobarbituric acid binding to malondialdehyde, formed a chromogenic complex during lipid peroxidation and the change in absorption peak was detected at 532 nm in a spectrophotometer. Additionally, the GSH activity was determined by the reaction of GSH with dithio-bis-nitrobenzoic acid (DTNB) to produce a product with a GSH assay kit. And the product could be measured using a spectrophotometer at 412 nm.

### **2.2.3. Histological examination by Van Gieson (VG) staining and Micro CT Scanning**

The distal femurs of the samples were scanned using Inveon micro-CT/PET (Siemens Medical Solutions, Germany) with 15 $\mu$ m resolution, and 80 kV tube voltage, 500 $\mu$ A tube current X-ray energy settings. The reconstruction and 3D quantitative analyses were conducted using Inveon research workplace 4.1 software. Similar settings for scans and analyses were applied for all of the samples. In the femur, the scanning regions were confined to the distal region, extending proximally 5.0 mm from the distal tip of the femoral condyle. The following bone indices in the defined region of interest (ROI) were analyzed: bone mineral density (BMD), trabecular thickness (Tb.Th), trabecular number (Tb.N), trabecular separation (Tb.Sp). The operator who conducted the scan analysis was blinded to the specimens.

Following Micro-CT scanning, the femur samples were decalcified in 10% EDTA with continuous shaking for 3 weeks. After dehydration and embedding, the distal femurs were embedded in paraffin. The sections were cut and stained with VG staining, which was used to stain for collagen fibers according to the manufacturer's instructions, The specimens were visualized, and pictures were taken with a high resolution microscope.

### **3. Statistical analysis**

The data are presented as the means  $\pm$  SD. The differences between two groups were probed using the Student's *t*-test. The differences among multiple groups were evaluated using a one-way ANOVA. Statistically significant results were indicated as \**P* < 0.05, \*\**P* < 0.01, #*P* < 0.05, and ##*P* < 0.01. Each experiment was repeated independently at least three times.

## **Results**

### **4.1 Cellular model of oxidative stress and curcumin protected from H<sub>2</sub>O<sub>2</sub>-induced cytotoxicity**

We established oxidative stress cell model by exposing to H<sub>2</sub>O<sub>2</sub> in vitro. We evaluated the level of oxidative stress in different H<sub>2</sub>O<sub>2</sub> concentration by measuring fluorescence signal with flow cytometry. Levels of intracellular ROS were increased with H<sub>2</sub>O<sub>2</sub> concentration during 24h (Fig 1A). The cell viability decreased dramatically after exposed to H<sub>2</sub>O<sub>2</sub> for 24 h at concentrations 300  $\mu$ M (Fig 1B). Curcumin alone at concentrations of 20  $\mu$ M or lower co-culture for 24 h did not influence on cell viability (Fig 1C). Importantly, 10  $\mu$ M or lower concentration of curcumin pretreatment before exposed to 0.3 mM H<sub>2</sub>O<sub>2</sub>

rescued cell viability, but this effect was not exist at the 20 $\mu$ m curcumin (Fig 1D). This result suggested that curcumin could partially inhibit H<sub>2</sub>O<sub>2</sub>-induced cytotoxicity below 10  $\mu$ M.

#### **4.2 curcumin reversed inhibition of osteogenic differentiation by H<sub>2</sub>O<sub>2</sub>**

ALP staining and activity were checked at 7 days, and calcium levels were evaluated at 21 days. We selected 0.3 mM H<sub>2</sub>O<sub>2</sub> for this experiment and chose the representative curcumin concentrations of 1, 10, 20  $\mu$ M in the study. The osteogenic medium containing curcumin were added after the cells were exposed to H<sub>2</sub>O<sub>2</sub> for 24 h. Co-culture of 1 and 10  $\mu$ M curcumin reversed H<sub>2</sub>O<sub>2</sub>-induced dysfunction, as indicated by increased ALP staining, activity and calcium level, but 20  $\mu$ M did not reverse the dysfunction (Fig 2A, 2B, 2C, 2D). 10 $\mu$ M curcumin treatment reversed H<sub>2</sub>O<sub>2</sub>-induced calcium level dysfunction dramatically, and 1  $\mu$ M treatment reversed the ALP activity markedly.

#### **4.3 Expression of IL-6 and RANKL was inhibited by curcumin**

Osteoblasts interact with osteoclasts synergistically to determine the metabolism of bone tissue. It is reported the osteoblasts always secrete several cell cytokines, which is critical to the activity of the osteoclasts in bone remodeling. IL-6 and RANKL are considered as two important cytokine secreted by osteoblasts. After exposure to 0.3 mM H<sub>2</sub>O<sub>2</sub> for 24 h, the levels of IL-6 and RANKL increased with 7 days induction. However, when co-cultured with curcumin, the elevated expression of RANKL and IL-6 was partially inhibited, especially at the 1  $\mu$ M and 10  $\mu$ M (Fig 3A, 3B).

#### **4.5.NF- $\kappa$ B signals are involved in the anti-oxidation**

As a common nuclear transcription factor in inflammation, NF- $\kappa$ B also plays an important role in regulating osteogenesis. The expression of the phosphorylated p65 subunit was increased when exposed to H<sub>2</sub>O<sub>2</sub>. Meanwhile, I $\kappa$ B- $\alpha$ , which is bound to the p65 subunit in the cytoplasm, was diminished. In contrast, curcumin (1  $\mu$ M) administration reduced the expression of p-P65 obviously but the 10, 20  $\mu$ M failed, conversely, the expression level of I $\kappa$ B- $\alpha$  in accordance with the p-P65. Therefore, curcumin conducted the protection from oxidation might be via the NF- $\kappa$ B signaling pathway (Fig 4A, 4B, 4C).

#### **4.6.Curcumin reduced oxidative stress in vivo**

Recently, oxidative stress is thought as the main pathological factor in the osteoporosis, so we employed the ovariectomized mouse model to study the protection of curcumin in vivo. To further study the effects of curcumin on oxidation in vivo, different amounts curcumin were administrate to the ovariectomized (OVX) mice intraperitoneally. Serum malondialdehyde (MDA) and glutathione (GSH) levels were varied in ovariectomized mice with or without curcumin intervention. The results found that the activity of MDA in serum increased but the GSH activity decreased in the ovariectomized group, and the serum activities of MDA and GSH were partially rescued by curcumin treatment (Fig 5A, 5B).

#### **4.7.Curcumin improved bone mass and bone structure in ovx mice**

The bone mass and micro-architecture were tested by VG staining and micro-computed tomography (micro-CT) examination. As shown in (Fig 6A), control mice had normal compact trabeculae in the femoral condyle, however sparse, thinned trabeculae were found in OVX mice with VG staining, curcumin treatment increased the thickness, density and the quantity of bone trabeculae. The bone mineral density and bone mass were quantified by micro-CT scanning (Fig 6B). Bone mass and bone trabeculae deteriorated in the vehicle group, as measured through decreases in BMD, Tb.N, Tb.Th (Fig 6C,D,E,F). Curcumin treatment improved the bone mineral density and micro-architecture in a dose-dependent manner. These results indicated that curcumin reversed the bone loss in vivo.

## Discussion

As we known, the oxidative stress was considered as main reason resulted in the osteoporosis currently, we employ the oxidative stress cell model to investigate the osteoporosis. In our experiments, we discovered that the viability of the cells was influenced by the concentration of the  $H_2O_2$ , lower viability with high  $H_2O_2$  concentration. We used the flow cytometer to detect the variation of the intracellular ROS, and found that the intracellular ROS augmented with the  $H_2O_2$  concentration, it reach top at the 300 $\mu$ M concentration during 24h, so we consider the  $H_2O_2$  could deduced much ROS co-cultured with cells for 24h. In the study of Leichnetz, they also measured the ROS of metals with flow cytometer<sup>[30]</sup>. Besides we investigate the toxicity of the  $H_2O_2$  and curcumin, 0.3mM  $H_2O_2$  impacted on the viability. Although 20 $\mu$ M curcumin have not influence on the viability, the 20 $\mu$ M curcumin could not rescued the viability of cells cultured with 300 $\mu$ M  $H_2O_2$ , so we decided employed the 0.3mM  $H_2O_2$  and 20 $\mu$ M curcumin in the study. Wang et al reported 0.2mM  $H_2O_2$  were used in their experiment, the  $H_2O_2$  co-cultured with human ASC<sup>[26]</sup>, but in Huang's experiment, they employed 0.3mM  $H_2O_2$ , they also used MC3T3-E1<sup>[31]</sup>. We also confirmed the low concentration of curcumin rescued the harms of  $H_2O_2$ . Although the 20 $\mu$ M curcumin have not toxicity on cells, the 20 $\mu$ M curcumin failed rescued the viability. The underlie mechanism does not clear, maybe the 20 $\mu$ M curcumin exerted the toxicity under  $H_2O_2$ . Many studies demonstrated that curcumin reversed the neurotoxic and behavioral damage in animal models of Alzheimer's disease (AD), which due to much ROS generation, and seems to be a promising molecule in prevention of AD<sup>[32]</sup>. Non-alcohol fatty liver disease (NAFLD) is closely related to oxidative stress, experiments suggested that curcumin exhibited better ameliorative effects in treating NAFLD<sup>[33]</sup>.

ALP activity and calcium content are main index of osteogenesis, alp is early biomarker of osteogenesis and calcium is late biomarker. In our study we not only measured the calcium content and alp activity but also staining, we found low concentration of curcumin protected the osteogenesis under oxidative stress. Kim et al found curcumin combined with BMP-2 facilitated bone tissue regeneration with up regulated alp and calcium content. We speculate the 1 $\mu$ M curcumin protected osteogenesis at early stage, and 10 $\mu$ M exerted late. Researchers have demonstrated the curcumin increased the rat MSC differentiated to osteoblast, with alp activity enhancement and mineralized nodule formation<sup>[34]</sup>.

The number and activity of osteoclasts increased significantly when the human marrow mononuclear cells cultured with  $H_2O_2$ <sup>[35]</sup>. The ligand of receptor activator of NF- $\kappa$ B (RANKL) and osteoprotegerin (OPG) were important regulator to osteoclast and osteoblast activity. The ratio of RANKL/OPG was sensitive to oxidative stress, and resulting in much bone resorption during the bone remodeling process<sup>[36-40]</sup>. Oxidative stress can also increase osteoclastogenesis through up-regulation of RANKL via the release of cytokines and prostaglandins<sup>[41, 42]</sup>. Osteoblast coordinated with osteoclast to decided osteoporosis or not, to some extent, the differentiation of osteoclast depended on the osteoblast. RANKL is an important factor which combined with rank promote maturation of the osteoclast<sup>[43]</sup>. Osteoblast also secreted inflammatory factor IL-6 regulated bone remodeling. Studies have confirmed that the concentration level of IL-6 and RANKL are high in the bone marrow of osteoporotic patients<sup>[44]</sup>. We found rankl and IL-6 in supernatant of culture, and confirmed that curcumin could reduced the level of the two factor. curcumin also considered as an anti-inflammatory agent. Studies also demonstrated that the antioxidant such as martine, Myricitrin, inhibits osteoclastogenesis through reduced IL-6 and RANKL expression, preventing bone loss<sup>[45, 46]</sup>, and the result demonstrated the curcumin exerted protection under the concentration of 10uM, and this is similar to the concentration attenuate the inhibition of osteogenesis from  $H_2O_2$ .

NF- $\kappa$ B signaling is a classic signal pathway in inflammation and oxidative stress<sup>[47]</sup>, numerous studies indicate that curcumin reversed the biologic process during inflammation and oxidation by reducing the activity of transcription factor NF- $\kappa$ B<sup>[48, 49]</sup>. Our studies demonstrated curcumin also reducing the expression of p-P65 and transcription of the phosphorylated factor. The concentration of 1uM exerted the suppression dramatically but high concentration failed. It is in accordance with the effect on IL-6 and RANKL. NF- $\kappa$ B signaling might be the potential pathway regulated the expression of IL-6 and RANKL, meanwhile affect the osteogenesis of the pre-osteoblast. The exact Glycyrrhizin was found to inhibited NF- $\kappa$ B signaling and decrease the secretion of inflammatory cytokines IL-6 and RANKL<sup>[50]</sup>. The curcumin exerted anti-oxidation and anti-inflammation together in this study, the oxidation also affected osteogenesis via inflammation factor generation. NF- $\kappa$ B signaling was considered as the main pathway participated in the osteogenesis when faced with inflammation<sup>[51, 52]</sup> and the curcumin facilitated osteogenesis via suppression the phosphorylation of P<sub>65</sub>.

In addition, in order to check the curcumin alleviated the oxidative stress in vivo or not, we employed the rat OVX model, which considered to mimic the osteoporosis classically. Malondialdehyde(MDA) is the product of lipid peroxidation by ROS; and glutathione (GSH), which removes free radicals, is regarded as an intracellular antioxidant, the quantity of the two index often represented the body redox state, Several studies have found that the production of MDA and GSH changed in the serum of postmenopausal women<sup>[53]</sup>. The production of MDA increased in the OVX group, might 1.6 times compared to control group, in contrast the quantity of GSH in OVX group reduce to 50% of control group. The curcumin reversed the ratio of MDA/GSH in treatment groups and in the dose dependence manner. Curcumin changed the total body redox state effectively. Next, we observed the architecture of the bone with VG staining and micro-CT scanning, found the micro-architecture of the trabecular bone dramatically

deteriorate in OVX, the trabecular bone become less and sparse, but in the curcumin group the trabecular bone architecture improved and depend on the dose of curcumin administrated. In order to qualified the trabecular bone, we measured the BMD, Tb.N, Tb.h of the femoral condyle, compared to the OVX group, the above index improved in treatment group in a dose manner, the bone architecture seem to compact in the 15  $\mu\text{mol/kg}$  group, this may attributed to the inhibition oxidative stress by curcumin facilitate the pre-osteoblast osteogenesis.

There are two limitation in our study, first, we have not employ the NF- $\kappa$ B signaling inhibitor to confirm the involved pathway.second, we have not measured the p-P65,IL-6, ranks in OVX bone.

## Conclusion

the oxidative stress inhibited the osteogenesis of osteoblast. Low concentrations of curcumin (1-10 $\mu\text{M}$ ) could reverse the inhibition, but a high concentration (20  $\mu\text{M}$ ) failed, the NF- $\kappa$ B signal might the main mechanism involved. Curcumin reversed the ratio of oxidants and antioxidants, and improved the bone micro-architecture of OVX, it was a candidate for osteoporosis treatment.

## Abbreviations

hydrogen peroxide	H <sub>2</sub> O <sub>2</sub>
alkaline phosphatase	ALP
malondialdehyde	MDA
glutathione	GSH
ovariectomized	OVX
bone mineral density	BMD
superoxide dismutase	SOD
N-acetyl-L-cysteine	NAC
methylthiazolyltetrazolium	MTS
p-nitrophenylphosphate	pNPP
dithio-bis-nitrobenzoic acid	DTNB
Van Gieson	VG
region of interest	ROI
Non-alcohol fatty liver disease	NAFLD
Alzheimer's disease	AD
osteoprotegerin	OPG

# Declarations

## Acknowledgements

We thank the Institute of The First Affiliated Hospital of Nanchang University, Nanchang for their support of this work.

## Authors' contributions

JiaQiang Xu and Qihua Qi developed the study design, performed the experiment, data analysis, and writing the manuscript. JiaQiang Xu, Ran Gao, Wen Liang, ChangJian Wu, FangLing Li, Sheng Huang, Bin Zhang and Qihua Qi, analyzed and interpreted the data. All authors read and approved the final manuscript.

## Funding

This research was supported by grants from National Natural Science Foundation of China (NO. 81960395)

## Availability of data and materials

The datasets used and analyzed in the study are available on request to the corresponding author.

## Declarations

Ethics approval and consent to participate

Not applicable.

## Consent for publication

Not applicable.

## Competing interests

The authors declare that they have no competing interests.

## Author details

Department of Orthopedic, The First Affiliated Hospital of Nanchang University, Nanchang

## Conflict of interest statement

The authors declare no conflict of interest.

# References

- [1] Lee S J, Graffy P M, Zea R D, et al. Future Osteoporotic Fracture Risk Related to Lumbar Vertebral Trabecular Attenuation Measured at Routine Body CT[J]. *J Bone Miner Res*, 2018,33(5):860-867.
- [2] Halling A, Persson G R, Berglund J, et al. Comparison between the Klemetti index and heel DXA BMD measurements in the diagnosis of reduced skeletal bone mineral density in the elderly[J]. *Osteoporos Int*, 2005,16(8):999-1003.
- [3] Ralston S H, Rizzoli R, Fielding R A. Calcified Tissue International-"the times, they are a-changin"[J]. *Calcif Tissue Int*, 2014,94(1):1.
- [4] He J, Xu S, Zhang B, et al. Gut microbiota and metabolite alterations associated with reduced bone mineral density or bone metabolic indexes in postmenopausal osteoporosis[J]. *Aging (Albany NY)*, 2020,12(9):8583-8604.
- [5] Delitala A P, Scuteri A, Doria C. Thyroid Hormone Diseases and Osteoporosis[J]. *J Clin Med*, 2020,9(4).
- [6] Seeman E, Delmas P D. Bone quality—the material and structural basis of bone strength and fragility[J]. *N Engl J Med*, 2006,354(21):2250-2261.
- [7] Lean J M, Jagger C J, Kirstein B, et al. Hydrogen peroxide is essential for estrogen-deficiency bone loss and osteoclast formation[J]. *Endocrinology*, 2005,146(2):728-735.
- [8] Aleman J O, Iyengar N M, Walker J M, et al. Effects of Rapid Weight Loss on Systemic and Adipose Tissue Inflammation and Metabolism in Obese Postmenopausal Women[J]. *J Endocr Soc*, 2017,1(6):625-637.
- [9] Chandra R V, Sailaja S, Reddy A A. Estimation of tissue and crevicular fluid oxidative stress marker in premenopausal, perimenopausal and postmenopausal women with chronic periodontitis[J]. *Gerodontology*, 2017,34(3):382-389.
- [10] Shen C L, Yang S, Tomison M D, et al. Tocotrienol supplementation suppressed bone resorption and oxidative stress in postmenopausal osteopenic women: a 12-week randomized double-blinded placebo-controlled trial[J]. *Osteoporos Int*, 2018,29(4):881-891.
- [11] Austermann K, Baecker N, Stehle P, et al. Putative Effects of Nutritive Polyphenols on Bone Metabolism In Vivo-Evidence from Human Studies[J]. *Nutrients*, 2019,11(4).
- [12] Baron R, Hesse E. Update on bone anabolics in osteoporosis treatment: rationale, current status, and perspectives[J]. *J Clin Endocrinol Metab*, 2012,97(2):311-325.
- [13] Kim R Y, Seong Y, Cho T H, et al. Local administration of nuclear factor of activated T cells (NFAT) c1 inhibitor to suppress early resorption and inflammation induced by bone morphogenetic protein-2[J]. *J Biomed Mater Res A*, 2018,106(5):1299-1310.

- [14] Karsenty G, Wagner E F. Reaching a genetic and molecular understanding of skeletal development[J]. *Dev Cell*, 2002,2(4):389-406.
- [15] Limgala R P, Goker-Alpan O. Effect of Substrate Reduction Therapy in Comparison to Enzyme Replacement Therapy on Immune Aspects and Bone Involvement in Gaucher Disease[J]. *Biomolecules*, 2020,10(4).
- [16] Arai M, Shibata Y, Pugdee K, et al. Effects of reactive oxygen species (ROS) on antioxidant system and osteoblastic differentiation in MC3T3-E1 cells[J]. *IUBMB Life*, 2007,59(1):27-33.
- [17] Lee D H, Lim B S, Lee Y K, et al. Effects of hydrogen peroxide (H<sub>2</sub>O<sub>2</sub>) on alkaline phosphatase activity and matrix mineralization of odontoblast and osteoblast cell lines[J]. *Cell Biol Toxicol*, 2006,22(1):39-46.
- [18] Jeong J W, Choi S H, Han M H, et al. Protective Effects of Fermented Oyster Extract against RANKL-Induced Osteoclastogenesis through Scavenging ROS Generation in RAW 264.7 Cells[J]. *Int J Mol Sci*, 2019,20(6).
- [19] Daniel S, Limson J L, Dairam A, et al. Through metal binding, curcumin protects against lead- and cadmium-induced lipid peroxidation in rat brain homogenates and against lead-induced tissue damage in rat brain[J]. *J Inorg Biochem*, 2004,98(2):266-275.
- [20] Morabito R, Falliti G, Geraci A, et al. Curcumin Protects -SH Groups and Sulphate Transport after Oxidative Damage in Human Erythrocytes[J]. *Cell Physiol Biochem*, 2015,36(1):345-357.
- [21] Kuo I M, Lee J J, Wang Y S, et al. Potential enhancement of host immunity and anti-tumor efficacy of nanoscale curcumin and resveratrol in colorectal cancers by modulated electro- hyperthermia[J]. *BMC Cancer*, 2020,20(1):603.
- [22] Kang H. MicroRNA-Mediated Health-Promoting Effects of Phytochemicals[J]. *Int J Mol Sci*, 2019,20(10).
- [23] Wan Q, Liu Z Y, Yang Y P, et al. Effect of curcumin on inhibiting atherogenesis by down-regulating lipocalin-2 expression in apolipoprotein E knockout mice[J]. *Biomed Mater Eng*, 2016,27(6):577-587.
- [24] Kowluru R A, Kanwar M. Effects of curcumin on retinal oxidative stress and inflammation in diabetes[J]. *Nutr Metab (Lond)*, 2007,4:8.
- [25] Liu Z, Ying Y. The Inhibitory Effect of Curcumin on Virus-Induced Cytokine Storm and Its Potential Use in the Associated Severe Pneumonia[J]. *Front Cell Dev Biol*, 2020,8:479.
- [26] Wang N, Wang F, Gao Y, et al. Curcumin protects human adipose-derived mesenchymal stem cells against oxidative stress-induced inhibition of osteogenesis[J]. *J Pharmacol Sci*, 2016,132(3):192-200.

- [27] Dai P, Mao Y, Sun X, et al. Attenuation of Oxidative Stress-Induced Osteoblast Apoptosis by Curcumin is Associated with Preservation of Mitochondrial Functions and Increased Akt-GSK3beta Signaling[J]. *Cell Physiol Biochem*, 2017,41(2):661-677.
- [28] Kim W K, Ke K, Sul O J, et al. Curcumin protects against ovariectomy-induced bone loss and decreases osteoclastogenesis[J]. *J Cell Biochem*, 2011,112(11):3159-3166.
- [29] Hussan F, Ibraheem N G, Kamarudin T A, et al. Curcumin Protects against Ovariectomy-Induced Bone Changes in Rat Model[J]. *Evid Based Complement Alternat Med*, 2012,2012:174916.
- [30] Lechnitz S, Heinrich J, Kulak N. A fluorescence assay for the detection of hydrogen peroxide and hydroxyl radicals generated by metallonucleases[J]. *Chem Commun (Camb)*, 2018,54(95):13411-13414.
- [31] Huang Q, Gao B, Jie Q, et al. Ginsenoside-Rb2 displays anti-osteoporosis effects through reducing oxidative damage and bone-resorbing cytokines during osteogenesis[J]. *Bone*, 2014,66:306-314.
- [32] Da C I, Freire M, de Paiva C J, et al. Supplementation with Curcuma longa Reverses Neurotoxic and Behavioral Damage in Models of Alzheimer's Disease: A Systematic Review[J]. *Curr Neuropharmacol*, 2019,17(5):406-421.
- [33] Feng W W, Kuang S Y, Tu C, et al. Natural products berberine and curcumin exhibited better ameliorative effects on rats with non-alcohol fatty liver disease than lovastatin[J]. *Biomed Pharmacother*, 2018,99:325-333.
- [34] Gu Q, Cai Y, Huang C, et al. Curcumin increases rat mesenchymal stem cell osteoblast differentiation but inhibits adipocyte differentiation[J]. *Pharmacogn Mag*, 2012,8(31):202-208.
- [35] Baek K H, Oh K W, Lee W Y, et al. Association of oxidative stress with postmenopausal osteoporosis and the effects of hydrogen peroxide on osteoclast formation in human bone marrow cell cultures[J]. *Calcif Tissue Int*, 2010,87(3):226-235.
- [36] Soltanoff C S, Yang S, Chen W, et al. Signaling networks that control the lineage commitment and differentiation of bone cells[J]. *Crit Rev Eukaryot Gene Expr*, 2009,19(1):1-46.
- [37] Fontani F, Marcucci G, Iantomasi T, et al. Glutathione, N-acetylcysteine and lipoic acid down-regulate starvation-induced apoptosis, RANKL/OPG ratio and sclerostin in osteocytes: involvement of JNK and ERK1/2 signalling[J]. *Calcif Tissue Int*, 2015,96(4):335-346.
- [38] Henriksen K, Neutzsky-Wulff A V, Bonewald L F, et al. Local communication on and within bone controls bone remodeling[J]. *Bone*, 2009,44(6):1026-1033.
- [39] Kamiya Y, Kikuchi T, Goto H, et al. IL-35 and RANKL Synergistically Induce Osteoclastogenesis in RAW264 Mouse Monocytic Cells[J]. *Int J Mol Sci*, 2020,21(6).

- [40] Xiao L, Zhou Y, Friis T, et al. S1P-S1PR1 Signaling: the "Sphinx" in Osteoimmunology[J]. *Front Immunol*, 2019,10:1409.
- [41] Graves D T, Alshabab A, Albiero M L, et al. Osteocytes play an important role in experimental periodontitis in healthy and diabetic mice through expression of RANKL[J]. *J Clin Periodontol*, 2018,45(3):285-292.
- [42] Xiao L, Zhou Y, Friis T, et al. S1P-S1PR1 Signaling: the "Sphinx" in Osteoimmunology[J]. *Front Immunol*, 2019,10:1409.
- [43] Hammerl A, Diaz C C, De-Juan-Pardo E M, et al. A Growth Factor-Free Co-Culture System of Osteoblasts and Peripheral Blood Mononuclear Cells for the Evaluation of the Osteogenesis Potential of Melt-Electrowritten Polycaprolactone Scaffolds[J]. *Int J Mol Sci*, 2019,20(5).
- [44] Pino A M, Rios S, Astudillo P, et al. Concentration of adipogenic and proinflammatory cytokines in the bone marrow supernatant fluid of osteoporotic women[J]. *J Bone Miner Res*, 2010,25(3):492-498.
- [45] Huang Q, Gao B, Wang L, et al. Protective effects of myricitrin against osteoporosis via reducing reactive oxygen species and bone-resorbing cytokines[J]. *Toxicol Appl Pharmacol*, 2014,280(3):550-560.
- [46] Chen X, Zhi X, Pan P, et al. Matrine prevents bone loss in ovariectomized mice by inhibiting RANKL-induced osteoclastogenesis[J]. *FASEB J*, 2017,31(11):4855-4865.
- [47] Zhang Z, Zhao H, Ge D, et al. beta-Casomorphin-7 Ameliorates Sepsis-Induced Acute Kidney Injury by Targeting NF-kappaB Pathway[J]. *Med Sci Monit*, 2019,25:121-127.
- [48] Huang F, Yao Y, Wu J, et al. Curcumin inhibits gastric cancer-derived mesenchymal stem cells mediated angiogenesis by regulating NF-kappaB/VEGF signaling[J]. *Am J Transl Res*, 2017,9(12):5538-5547.
- [49] Cao J, Ye B, Lin L, et al. Curcumin Alleviates oxLDL Induced MMP-9 and EMMPRIN Expression through the Inhibition of NF-kappaB and MAPK Pathways in Macrophages[J]. *Front Pharmacol*, 2017,8:62.
- [50] Li Z, Chen C, Zhu X, et al. Glycyrrhizin Suppresses RANKL-Induced Osteoclastogenesis and Oxidative Stress Through Inhibiting NF-kappaB and MAPK and Activating AMPK/Nrf2[J]. *Calcif Tissue Int*, 2018,103(3):324-337.
- [51] Zhang A, Zhang X, Tan X, et al. Resveratrol rescued the TNF-alpha-induced impairments of osteogenesis of bone-marrow derived mesenchymal stem cells and inhibited the TNF-alpha-activated NF-small ka, CyrillicB signaling pathway[J]. *Int Immunopharmacol*, 2015,26(2):409-415.
- [52] Liu Y, Fang S, Li X, et al. Aspirin inhibits LPS-induced macrophage activation via the NF-kappaB pathway[J]. *Sci Rep*, 2017,7(1):11549.

[53] Ozgocmen S, Kaya H, Fadillioglu E, et al. Role of antioxidant systems, lipid peroxidation, and nitric oxide in postmenopausal osteoporosis[J]. Mol Cell Biochem, 2007,295(1-2):45-52.

## Figures

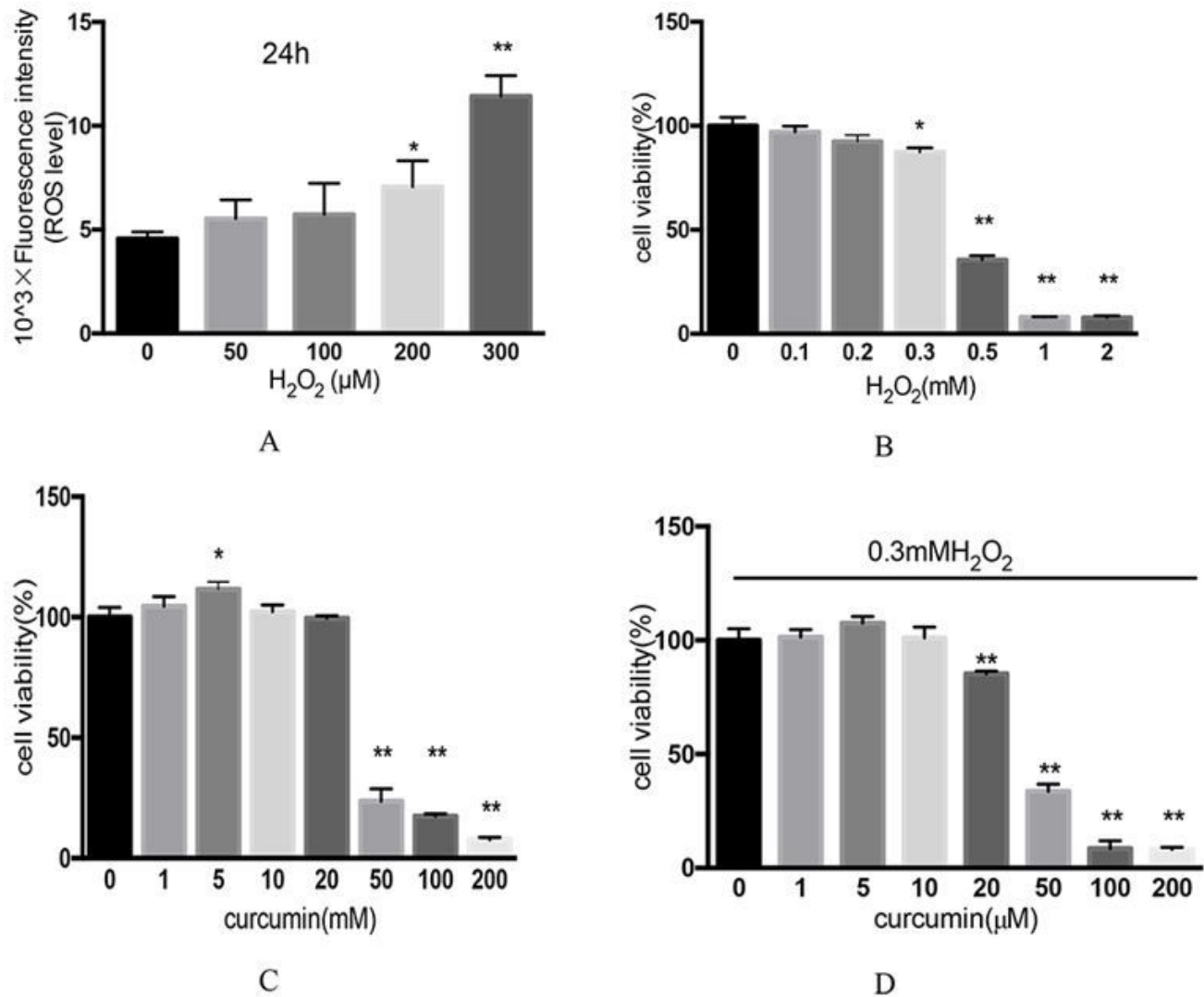
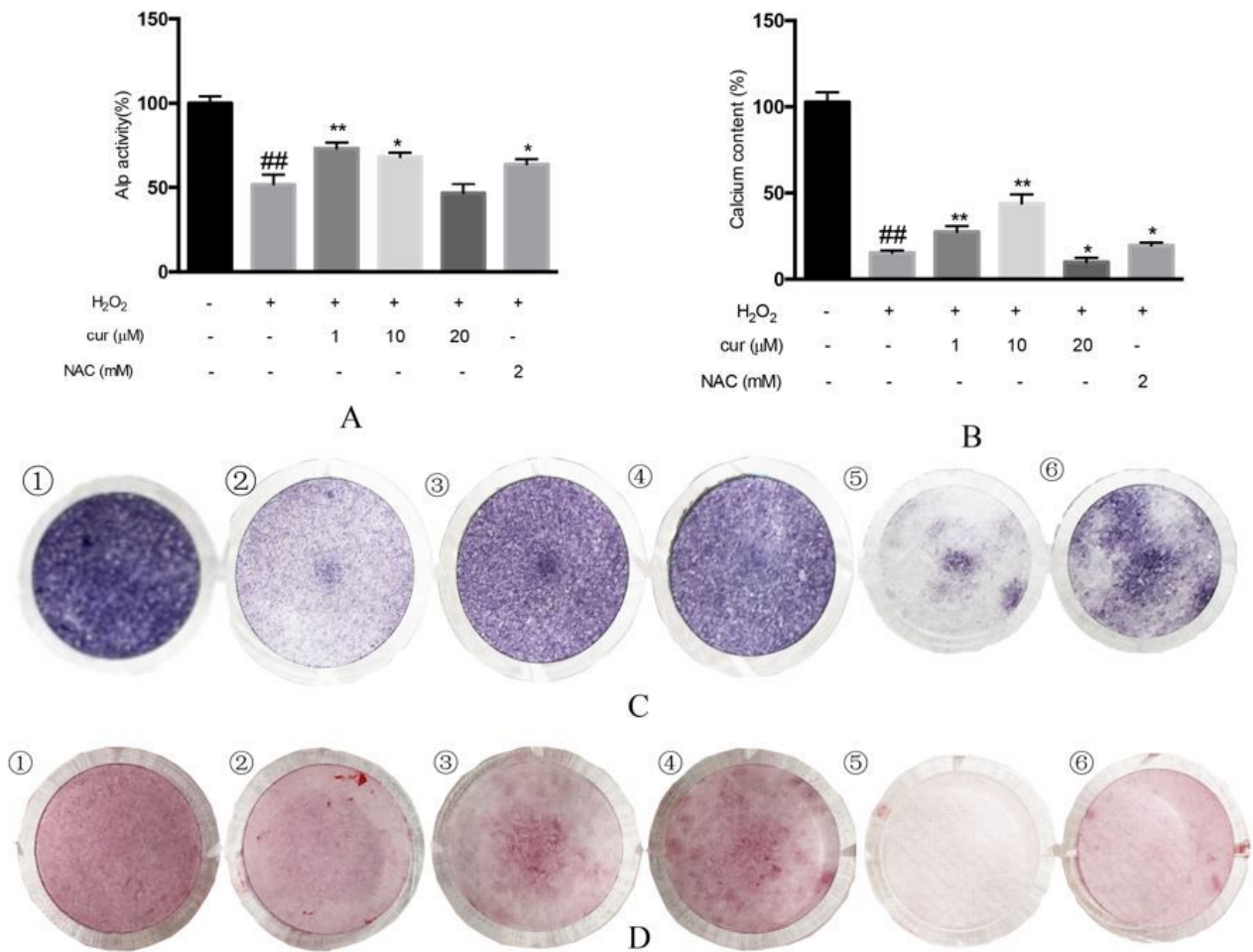


Figure 1

Intracellular ROS after exposed to H<sub>2</sub>O<sub>2</sub> and the cell viability of different concentrations H<sub>2</sub>O<sub>2</sub> or curcumin. Data are presented as the means  $\pm$  S.E.M. \*p < 0.05 and \*\*p < 0.01 versus control.



**Figure 2**

Curcumin protected cells osteogenesis from H<sub>2</sub>O<sub>2</sub> exposure. A, B. ALP activity and the calcium content with different concentrations curcumin treatment C, D ALP and Alizarin Red S staining with different concentrations curcumin treatment ☐: Control; ☐: H<sub>2</sub>O<sub>2</sub>; ☐: H<sub>2</sub>O<sub>2</sub>+cur (1 μM); ☐: H<sub>2</sub>O<sub>2</sub>+cur (10 μM); ☐: H<sub>2</sub>O<sub>2</sub>+cur (20 μM); ☐: H<sub>2</sub>O<sub>2</sub>+NAC (2 mM). ##p < 0.01 compared with the control group; \*p < 0.05 and \*\*p < 0.01 compared to the H<sub>2</sub>O<sub>2</sub> group.

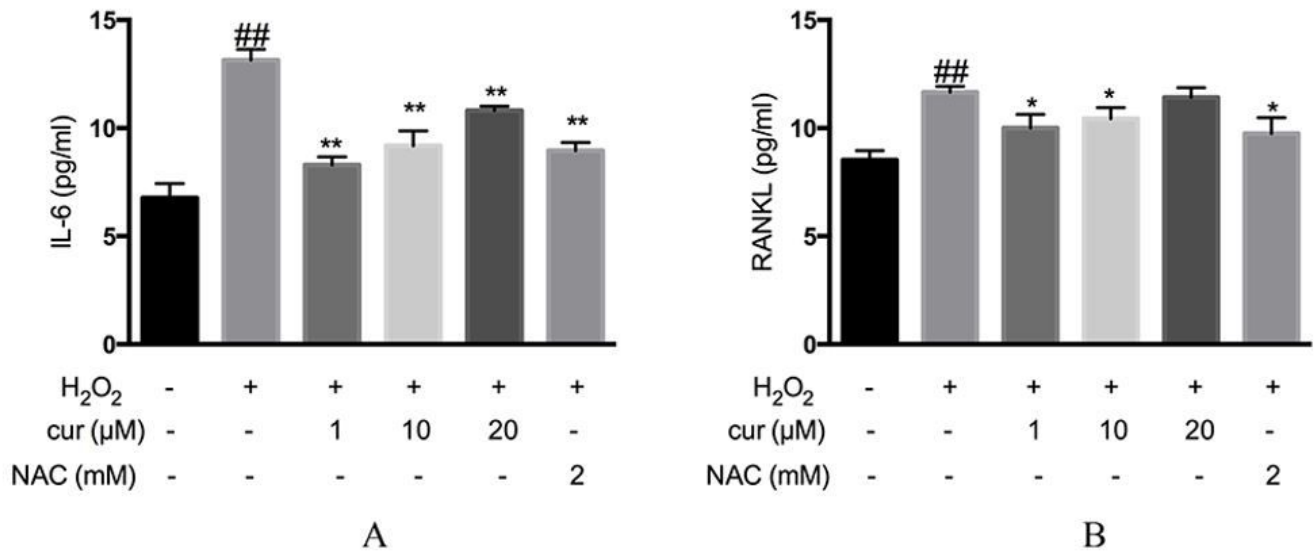


**Figure 3**

Curcumin down-regulated the level of IL-6 and RANKL. \*P < 0.05 and \*\*P < 0.01 in contrast to the H<sub>2</sub>O<sub>2</sub> alone treatment group, ##P < 0.01 compared with the control group.

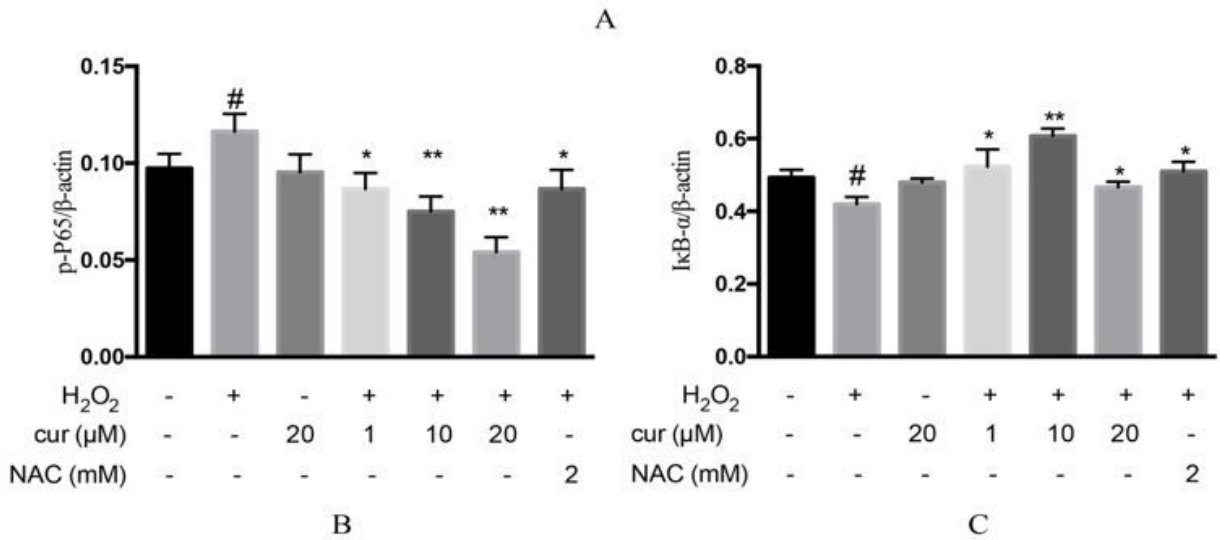
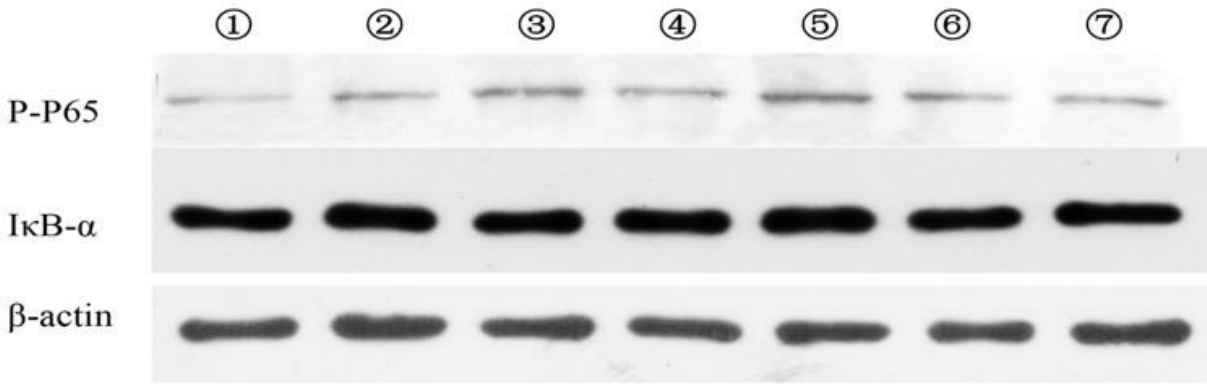


**Figure 4**

NF-κB pathways are involved in the curcumin-mediated anti-oxidation. 4A, 4B, 4C Western blot analysis and relative protein quantification of p-p65 and IκB-α. □: control group; ▤: Cur 20μM; ▥: H<sub>2</sub>O<sub>2</sub>; ▦: H<sub>2</sub>O<sub>2</sub>+cur (1 μM); ▧: H<sub>2</sub>O<sub>2</sub>+cur (10 μM); ▨: H<sub>2</sub>O<sub>2</sub>+cur (20 μM); ▩: H<sub>2</sub>O<sub>2</sub>+NAC (2 mM). Data are shown as the means ± S.E.M. \*p < 0.05 and \*\*p < 0.01 versus H<sub>2</sub>O<sub>2</sub>-treatment group; #p < 0.05 and ##p < 0.01 versus control group.

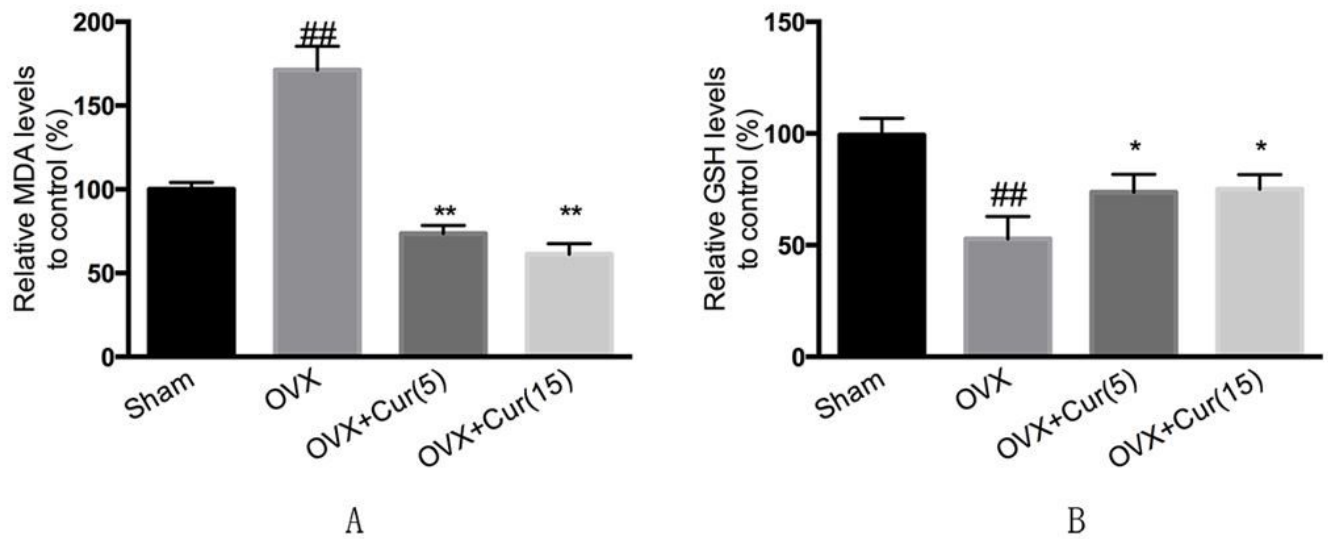


**Figure 5**

Curcumin attenuates the expression of MDA and GSH in vivo. \* $P < 0.05$  and \*\* $P < 0.01$  compared to the OVX group, ## $P < 0.01$  compared with the sham group.

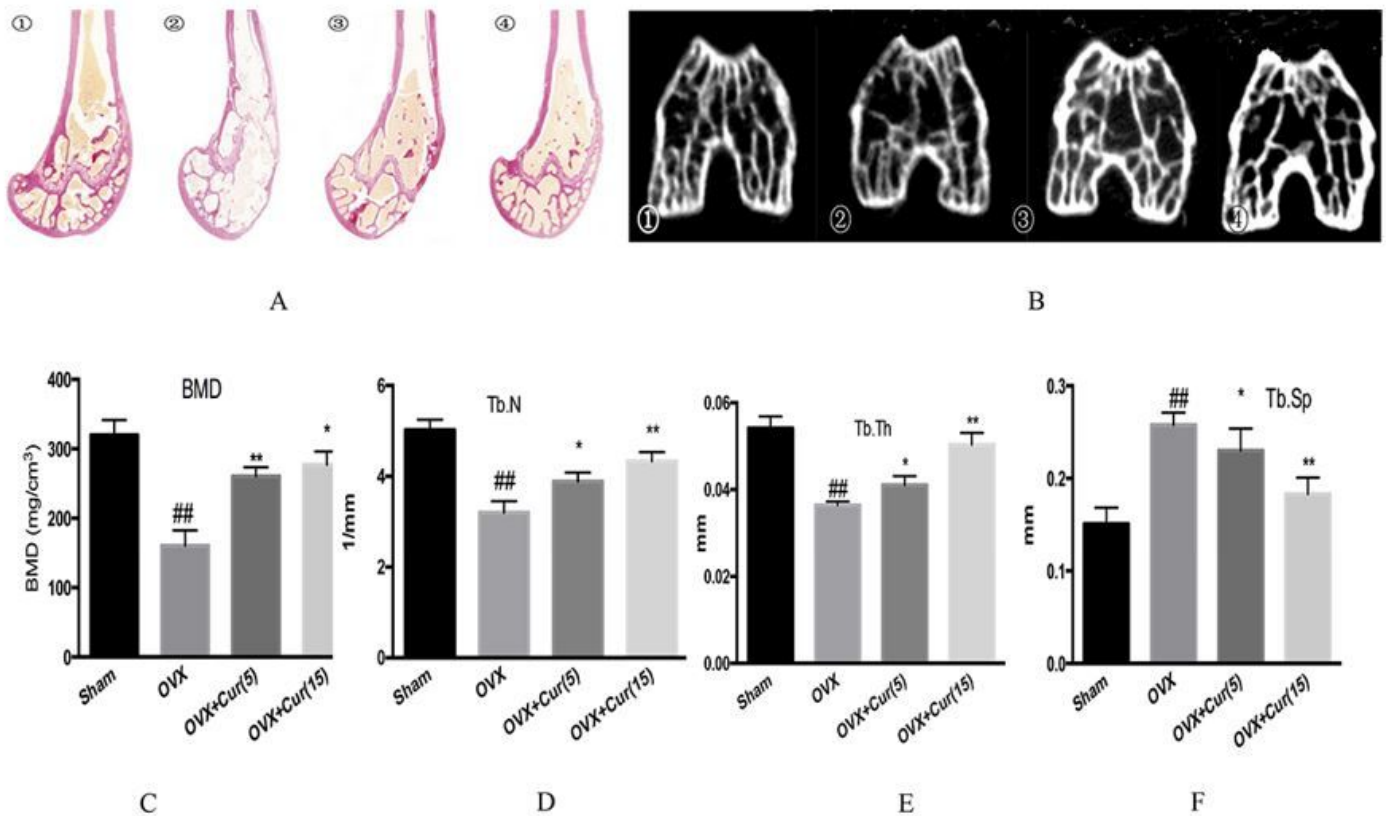


**Figure 6**

curcumin reversed bone harms in OVX animal model. □: sham group; □: OVX; □: OVX+cur (5 μmol/kg); □: OVX +cur (15 μmol/kg)